



Alterations in metabolic pathways in gastric epithelial cells infected with *Helicobacter pylori*

Matsunaga, Shinsuke

Nishiumi, Shin

Tagawa, Ryoma

Yoshida, Masaru

(Citation)

Microbial Pathogenesis, 124:122-129

(Issue Date)

2018-11

(Resource Type)

journal article

(Version)

Accepted Manuscript

(Rights)

© 2018 Elsevier.

This manuscript version is made available under the CC-BY-NC-ND 4.0 license

<http://creativecommons.org/licenses/by-nc-nd/4.0/>

(URL)

<https://hdl.handle.net/20.500.14094/90005593>



Alterations in metabolic pathways in gastric epithelial cells infected with
Helicobacter pylori

Shinsuke Matsunaga^a, Shin Nishiumi^{a,*}, Ryoma Tagawa^a, Masaru Yoshida^{a,b,c,*}

^aDivision of Gastroenterology, Department of Internal Medicine, Kobe University
Graduate School of Medicine, Kobe, Japan.

^bDivision of Metabolomics Research, Department of Internal Related, Kobe University
Graduate School of Medicine, Kobe, Japan.

^cAMED-CREST, AMED, Kobe, Japan.

*Corresponding author: Division of Gastroenterology, Department of Internal Medicine,
Kobe University Graduate School of Medicine, 7-5-1 Kusunoki-cho, Chu-o-ku, Kobe,
Hyogo 650-0017, Japan.

Phone: +81-78-382-6305; Fax: +81-78-382-6309

E-mail: nishiums@med.kobe-u.ac.jp (SN) & myoshida@med.kobe-u.ac.jp (MY)

Abstract

Helicobacter pylori (*H. pylori*), which is a spiral-shaped Gram-negative microaerobic bacterium, is a causative pathogen. The entry of *H. pylori* into gastric epithelial cells involves various host signal transduction events, and its virulence factors can also cause a variety of biological responses. In this study, AGS human gastric carcinoma cells were infected with CagA-positive *H. pylori* strain ATCC43504, and then the metabolites in the AGS cells after the 2-, 6- and 12-hour infections were analyzed by GC/MS-based metabolomic analysis. Among 67 metabolites detected, 11 metabolites were significantly altered by the *H. pylori* infection. The metabolite profiles of *H. pylori*-infected AGS cells were evaluated on the basis of metabolite pathways, and it was found that glycolysis, tricarboxylic acid (TCA) cycle, and amino acid metabolism displayed characteristic changes in the *H. pylori*-infected AGS cells. At 2 hour post-infection, the levels of many metabolites related to TCA cycle and amino acid metabolism were lower in *H. pylori*-infected AGS cells than in the corresponding uninfected AGS cells. On the contrary, after 6-hour and 12-hour infections the levels of most of these metabolites were higher in the *H. pylori*-infected AGS cells than in the corresponding uninfected AGS cells. In addition, it was shown that the *H. pylori* infection might regulate the pathways related to isocitrate dehydrogenase and asparagine synthetase. These metabolite alterations in gastric epithelial cells might be involved in *H. pylori*-induced biological responses; thus, our findings are important for understanding *H. pylori*-related gastric diseases.

Keywords

Helicobacter pylori; metabolomics; GC/MS.

42

43 **Abbreviations**

44 *H. pylori*, *Helicobacter pylori*; MALT, mucosa-associated lymphoid tissue; IARC,
45 International Agency for Research on Cancer; CagA, cytotoxin-associated protein A;
46 *cagPAI*, *cag* pathogenicity island; VacA, vacuolating cytotoxin A; GC/MS, gas
47 chromatography/mass spectrometry; FBS, fetal bovine serum; PBS, phosphate-buffered
48 saline; DMSO, dimethyl sulfoxide; TNF- α , tumor necrosis factor alpha; IL-8,
49 interleukin 8; IDH, isocitrate dehydrogenase; ASNS, asparagine synthetase; SEM,
50 standard error of the mean; TCA, tricarboxylic acid; NAD, nicotinamide adenine
51 dinucleotide; NADP, nicotinamide adenine dinucleotide phosphate; CoA, coenzyme A.

52

1. Introduction

Helicobacter pylori (*H. pylori*) is a spiral-shaped Gram-negative microaerobic bacterium. About half of the global population is infected with *H. pylori*, making it the most widespread infection in the world. It had been believed that no bacterium can colonize the stomach because of the presence of gastric acid, and *H. pylori* was not detected in the stomach for a long time due to the difficulty in culturing it *in vitro*. However, B. Marshall and R. Warren reported the isolation of this bacterium from patients with chronic gastritis or peptic ulcers [1], and a variety of studies of *H. pylori* have since been performed. *H. pylori*, which can inhabit the stomach as it produces a potent urease that neutralizes gastric acid, is a causative pathogen of gastric adenocarcinoma, chronic gastritis, peptic ulcers, and mucosa-associated lymphoid tissue (MALT) lymphoma. *H. pylori* was also classified as a group 1 carcinogen by the International Agency for Research on Cancer (IARC) [2]. The invasion of *H. pylori* into the gastric epithelial cells induces various host signal transduction events [3], and its virulence factors can also cause a variety of biological responses. In addition, *H. pylori* is involved in some extragastric diseases. For example, recent studies have revealed that it is associated with diabetes mellitus and cardiovascular neurological, autoimmune, hepatobiliary, colonic, and pancreatic diseases [4]. Therefore, *H. pylori* virulence factors became an important focus of research. Among these virulence factors, cytotoxin-associated protein A (CagA) is the most extensively studied, and its gene is encoded within the *cag* pathogenicity island (*cagPAI*). In Western countries, *cagA*-positive *H. pylori*-infected individuals were found to be at higher risk of peptic ulcers or gastric cancer than *cagA*-negative *H. pylori*-infected individuals [5]. The CagA protein is injected into the epithelial cells of the host via the type IV secretion system,

77 and it activates or inactivates multiple signaling pathways via both
78 phosphorylation-dependent and phosphorylation-independent mechanisms [6,7]. There
79 are more than 20 known cellular binding partners of CagA [6], and CagA regulates cell
80 proliferation, motility, and polarity, which modulate the phenotypes of host cells [8].
81 Vacuolating cytotoxin A (VacA), which is the second most extensively studied virulence
82 factor, is a secreted bacterial toxin. VacA induces membrane-channel formation;
83 cytochrome *c* release from mitochondria, leading to apoptosis; and binding to
84 cell-membrane receptors after pro-inflammatory responses, and it also inhibits T-cell
85 activation and proliferation [9]. Although there have been numerous studies of *H. pylori*
86 virulence factors, it remains to be fully elucidated why the diseases caused by *H. pylori*
87 infections (which involve a single bacterial species) exhibit such marked diversity.

88

89 Recently, genomic and proteomic approaches have been used to study *H. pylori*
90 infections. In the article by Backert S et al., the mRNA profiling and protein profiling in
91 AGS cells were performed to characterize the temporal response of gastric epithelial
92 cells to the *H. pylori* infection and to evaluate the contributions of the *cag* PAI-encoded
93 type IV secretion system to the host responses, and it was suggested that *H. pylori*
94 interacts with the dynamic cytoskeleton of host in causing the motogenic responses and
95 cellular elongation [10]. In addition, the phosphoproteome of AGS cells infected with *H.*
96 *pylori* was analyzed, and it was shown that *H. pylori* affects several factors involved in
97 pre-mRNA processing and alternative splicing control [11]. However, we have not yet
98 obtained a complete understanding of *H. pylori*'s pathogenic diversity, especially from
99 the viewpoint of metabolism. Therefore, in this study, metabolomics was used to
100 investigate *H. pylori* infections. Metabolomics or metabolomic analysis involves the

comprehensive study of low-molecular-weight metabolites in the body and is considered to explain the status of cells in more detail than other omics techniques because the metabolome is located downstream of DNA, RNA, and proteins, and it is closer to the phenotype [12]. This study tried to acquire novel findings about *H. pylori* infections via *in vitro* infection experiments. AGS human gastric carcinoma cells were infected with the CagA-positive *H. pylori* strain ATCC43504, and then the metabolites in the infected AGS cells were analyzed using gas chromatography/mass spectrometry (GC/MS)-based metabolomics.

2. Materials and methods

2.1. Bacteria

The CagA-positive and VacA-positive *H. pylori* strain ATCC43504 was cultured on trypticase soy agar II with 5% sheep blood (Nippon Becton Dickinson, Tokyo, Japan) under microaerobic conditions (5% O₂, 5% CO₂, and 90% N₂) at 37°C. Before each experiment, *H. pylori* was grown overnight in Brucella broth (BD Biosciences, Franklin Lakes, NJ, USA) supplemented with 10% inactivated fetal bovine serum (FBS) (Life Technologies Corporation, Carlsbad, CA, USA) under microaerobic conditions at 37°C while being shaken at 250 rpm.

2.2. Cells

AGS human gastric carcinoma cells were maintained in RPMI1640 medium (WAKO, Osaka, Japan) supplemented with 10% inactivated FBS. AGS cells were serum-starved for 16 hours, before they were infected with *H. pylori* at a multiplicity of infection (MOI) of 200:1 for the indicated times. When AGS cells were infected with *H. pylori*,

their levels of confluency were 60-70%. The AGS cells after the *H. pylori* infection at MOI of 200:1 were hardly dead, because almost cells were attached to the cell culture dishes, and the number of cells was not also decreased compared with the control cells. The morphological changes in the *H. pylori*-infected AGS cells were observed using a microscope in a blinded manner, and the ratio of the cells with the typical elongation phenotype was evaluated by calculating the numbers of cells with and without the typical elongation phenotype. The numbers of cells with and without the typical elongation phenotype were counted for 3 fields per 1 culture dish, and then the results of the ratio from these three viewpoints were averaged to be the value of 1 culture dish. The 3 independent experiments were performed for each group.

2.3. GC/MS analysis

The cells were harvested at 2, 6, or 12 hours after being infected at a multiplicity of infection of 200:1. To do this, they were washed twice with phosphate-buffered saline (PBS), before being scraped and then centrifuged at 200 x g for 5 minutes at 4°C. The resultant cell pellets were suspended in 1 mL of PBS, and then the number of cells was counted. After the suspension had been centrifuged at 400 x g for 5 minutes at 4°C, the supernatant was removed, and the cell pellet was washed with distilled water once. Extraction of low-molecular-weight metabolites from the cells and the following GC/MS analysis were performed according to the method described in a previous report [13,14]. For semi-quantification, the peak height of each ion was calculated and normalized using the peak height of 2-isopropylmalic acid as an internal standard and the number of cells.

2.4. Proteasome inhibition study

AGS cells were serum-starved for 16 hours, and then the cells were pre-incubated with 0.5 μ M MG132 (Sigma-Aldrich, St. Louis, MO, USA) dissolved in dimethyl sulfoxide (DMSO) (WAKO, Osaka, Japan) for 30 minutes, before being infected with *H. pylori* for 12 hours at a multiplicity of infection of 200:1. Then, the target mRNA level was evaluated via the real-time PCR. The cells were also subjected to the preparation for GC/MS analysis.

2.5. Real-time PCR

AGS cells were plated at a density of 2.0×10^6 cells/100-mm plate or 2.0×10^5 cells/well on the 6-well plate before being used in each experiment. Total RNA was extracted with TRIzol reagent (Life Technologies Corporation, Carlsbad, CA, USA). Reverse transcription was performed with a high capacity cDNA reverse transcription kit (Applied Biosystems, Tokyo, Japan) or RT² First Strand Kit (Qiagen, Germantown, MD, USA). mRNA expression levels were evaluated using a real-time PCR system and power SYBR green PCR master mix (Applied Biosystems, Tokyo, Japan). The expression levels of the target mRNA were normalized to that of β -actin. The primer sequences used were as follows: tumor necrosis factor alpha (TNF- α) (forward: 5'-CCCATGTTGTAGCAAACCCTC-3'; reverse: 5'-TATCTCTCAGCTCCACGCCA-3'), interleukin 8 (IL-8) (forward: 5'-AAGAAACCACCGGAAGGAAC-3'; reverse: 5'-ACTCCTTGGCAAACTGCAC-3'), β -actin (forward: 5'-AAATCTGGCACCACACCTTC-3'; reverse: 5'-TGATCTGGGTCATCTTCTCG-3'),

isocitrate dehydrogenase 1 (IDH1) (forward: 5'-CTGTGGCCCAAGGGTATGG-3';
reverse: 5'-CATGCGGTAGTGACGGGTTA-3'), IDH2 (forward:
5'-ACAACACCGACGAGTCCATC-3'; reverse: 5'-GCCCATCGTAGGCTTTCAGT-3'),
IDH3 (forward: 5'-CTCTAAGGTCTCTCGGCTGC-3'; reverse:
5'-GGGCCAATACCATCTCCTGG-3'), asparagine synthetase (ASNS) (forward:
5'-ACGCCCTCTATGACAATGTG-3'; reverse:
5'-TCCAAGCCCCCTGATAAAAG-3').

2.6. Short interfering RNA experiment

ASNS siRNA (#1: s1678, #2: s1679; Thermo Fisher Scientific, Waltham, MA, USA)
and the control siRNA (Thermo Fisher Scientific, Waltham, MA, USA) were dissolved
in RNase-free water to produce a 10 μ M solution. AGS cells were plated at a density of
 2×10^5 cells/well on the 6-well plate, and then were cultured for 24 hours. Four μ L of
Lipofectamine 2000 (Thermo Fisher Scientific, Waltham, MA, USA) was mixed with 1
mL of Opti-MEM (Thermo Fisher Scientific, Waltham, MA, USA) for 5 minutes at
37°C, and then the siRNA solution were added into the prepared Lipofectamine 2000
solution, followed by incubation for 5 minutes at 37°C. Next, AGS cells were treated
with the mixture for 48 hours. The cells were infected with *H. pylori* for the last 18
hours of 48 hours at a multiplicity of infection of 200:1.

2.7. Western blotting

AGS cells infected with *H. pylori* at a multiplicity of infection of 200:1 were harvested
with a lysis buffer (50 mM Tris-HCl (pH 8.0), 150 mM NaCl, 1% NP-40, 0.5% sodium
deoxycholate, 0.1% sodium dodecyl sulfate) containing phosphatase inhibitors and

protease inhibitors, and then the cell solutions were incubated at 4°C for 30 minutes with mixing. The solutions were centrifuged at $15,000 \times g$ for 20 minutes at 4°C, and the supernatant obtained was used as a cell lysate, followed by immunoprecipitation and Western blotting. For immunoprecipitation and Western blotting, agarose-conjugated anti-phosphotyrosine antibody (Millipore, Bedford, MA, USA), anti-CagA antibody (Austral Biologicals, San Ramon, CA, USA), β -actin antibody (Sigma-Aldrich, St. Louis, MO, USA), and anti-ASNS antibody (Merk, Temecula, CA, USA) were purchased.

2.8. IDH activity experiment

AGS cells were harvested at 6 or 12 hours after being infected at a multiplicity of infection of 200:1. After being washed with PBS twice, the cells were subjected to an isocitrate dehydrogenase assay (Abcam, Cambridge, United Kingdom).

2.9. Statistical analysis

The results are expressed as the mean \pm standard error of the mean (SEM). The statistical significance of differences was analyzed using the Student's t-test, and a probability level of 0.05 was used as the criterion for significance.

3. Results

In this study, AGS human gastric carcinoma cells were infected with *H. pylori* strain ATCC43504, which possesses Western-type CagA and s1a-m1-type VacA virulence factors. In our experiment using *H. pylori* strain ATCC43504, the significant

upregulation of IL-8 and TNF- α could not be observed in the AGS cells infected with *H. pylori* at MOI of 50:1, and the increased levels of IL-8 and TNF- α by the *H. pylori* infection at MOI of 100:1 was low (**Fig. S1**). Therefore, we selected MOI of 200:1 as the experiment for our metabolomic study about *H. pylori*. **Fig. 1(A)** shows photographs obtained during microscopic examinations of the AGS cells at 6 or 12 hours after the cells were infected with *H. pylori* as well as images of the corresponding uninfected cells. At 6 hour post-infection, we could observe a few morphological changes in the AGS cells, and the ratio of the cells with the typical elongation phenotype was 40.0%. Some cells exhibited the altered morphologies at 12 hour post-infection, and the ratio of the cells with the typical elongation phenotype was 68.8%. The ratio at the 12 hour post-infection was significantly higher than the 6 hour post-infection. In **Fig. 1(B)**, CagA was detected in the AGS cells infected with *H. pylori*, and phosphorylation of CagA could be also confirmed, and the same results were observed at our previous study using the same *H. pylori* strain (ATCC43504) [15]. These results indicate that CagA was translocated into AGS cells via the type IV secretion system.

Next, the metabolites in the *H. pylori*-infected AGS cells were analyzed via GC/MS-based metabolomic analysis, and then the relationships between *H. pylori* infection and metabolite alterations were evaluated. In our GC/MS-based metabolomic analysis, 67 metabolites were detected (**Table S1**). At 2 hour post-infection, asparagine was the only metabolite whose level was significantly altered (the infected cells demonstrated significantly lower asparagine levels than the corresponding uninfected AGS cells) (**Table 1**). At 6 hour post-infection, the infected cells displayed

significantly higher levels of 2-aminopimelic acid, citric acid+isocitric acid, valine, and malic acid and significantly lower levels of asparagine and 1,6-anhydroglucose than the corresponding uninfected AGS cells (**Table 1**). At 12 hour post-infection, the infected cells exhibited significantly higher levels of citric acid+isocitric acid, serine, glycine, threonine, taurine, valine, and 2-aminoethanol than the corresponding uninfected AGS cells (**Table 1**).

Then, the metabolite profiles of the AGS cells that were infected with *H. pylori* were evaluated on the basis of metabolite pathways (**Fig. S2**). The metabolite pathways shown in **Fig. S2** were generated according to the KEGG database (<https://www.genome.jp/kegg/>). In **Fig. S2**, red and blue colors indicate that the level of the metabolite was higher and lower, respectively, in the *H. pylori*-infected AGS cells than in the uninfected controls. As a result, it was found that glycolysis, the tricarboxylic acid (TCA) cycle and the associated amino acid metabolic pathways exhibited characteristic changes in the *H. pylori*-infected AGS cells, although most of the metabolites related to glycolysis could not be detected in this study. At 2 hour post-infection, the levels of many metabolites related to the TCA cycle and the associated amino acid metabolism were lower in the infected AGS cells than in the corresponding uninfected AGS cells. On the contrary, at 6 hour and 12 hour post-infection, the levels of most of these metabolites were higher in the infected AGS cells than in the corresponding uninfected AGS cells.

Based on the glycolysis, TCA cycle, and amino acid metabolism-related metabolite profiles seen in the *H. pylori*-infected AGS cells, we decided to focus on asparagine,

because its level in the infected AGS cells was lower than those seen in the corresponding uninfected AGS cells during all infection periods examined in this study (**Table S1**; **Fig. S2**). Asparagine is generated from aspartic acid by ASNS (**Fig. S3**). Therefore, the reduced level of asparagine seen in the *H. pylori*-infected AGS cells might have been caused by the inactivation of ASNS, possibly leading to affecting the biological responses to the *H. pylori* infection. In this study, the siRNA knockdown of ASNS mRNA was performed, and ASNS protein was silenced in AGS cells (**Fig. 2(A)**). The decline in ASNS mRNA was also observed in the AGS cells treated with ASNS siRNA (data not shown). In these experimental conditions using 100 pmols ASNS siRNA, we investigated whether ASNS downregulation affects the *H. pylori* infection-induced upregulation of IL-8 expression. As a result, the level of ASNS tended to be increased in the *H. pylori*-infected AGS cells compared with the non-infected AGS cells without the significant difference ($p=0.069$). The ASNS downregulation suppressed the *H. pylori* infection-induced IL-8 upregulation in AGS cells (**Fig. 2B**).

As shown in **Fig. S2**, at 6 and 12 hour post-infection most amino acids exhibited higher levels in the infected AGS cells than in the corresponding uninfected AGS cells. These increases in the levels of various amino acids might have been induced by the upregulation of protein degradation in the *H. pylori*-infected AGS cells, which is dependent on the amino acid requirement. Therefore, AGS cells were treated with MG132, which is an inhibitor of proteasomes and calpains, or DMSO as a vehicle control, and then were infected with *H. pylori*, before being subjected to evaluations of TNF- α and IL-8 mRNA expression (**Fig. 3**). The treatment concentration of MG132 (10

μM) was decided according to the previous report by Fan XM *et al.* [16], because, AGS cells were treated with 10 μM MG132 in the experiments by Fan XM *et al.*, and it was shown that its concentration (10 μM) can inhibit the ubiquitin-proteasome pathway. As a result, it was found that MG132 inhibited the increases in TNF-α and IL-8 mRNA expression induced by *H. pylori*.

Next, it was investigated how the levels of metabolites evaluated in **Fig. S2** altered in the AGS cells with MG132 (**Table S2**). In the uninfected AGS cells, MG132 increased the levels of most of the evaluated metabolites in comparison to DMSO as a vehicle control. Then, the similar results were observed the *H. pylori*-infected AGS cells with and without the MG132 treatment, and the *H. pylori*-induced increases in the levels of targeted metabolites were not cancelled by the MG132 treatment.

As shown in **Table 1** and **Table S1**, the level of citric acid/isocitric acid in the AGS cells was increased at 6 and 12 hour post-infection. The level of citric acid/isocitric acid in the cells is regulated by IDH, which includes 3 isoforms: IDH1, IDH2, and IDH3. Therefore, the mRNA expression levels of IDH1, IDH2, and IDH3a in the *H. pylori*-infected AGS cells were evaluated (**Fig. 4**). As a result, it was shown that there were no marked alterations in their mRNA expression levels at 6 or 12 hour post-infection, although their mRNA expression levels tended to be decreased at 6 hour post-infection. Next, the enzymatic activity of IDH in the *H. pylori*-infected AGS cells was evaluated (**Fig. 4**). In this study, the influence of *H. pylori* infection on the enzymatic activity of nicotinamide adenine dinucleotide (NAD)⁺-dependent IDH and nicotinamide adenine dinucleotide phosphate (NADP)⁺-dependent IDH were

investigated. Regarding NAD⁺-dependent IDH, its enzymatic activity was significantly reduced at 6 and 12 hour post-infection. NADP⁺-dependent IDH activity was significantly reduced at 12 hour post-infection.

4. Discussion

H. pylori infections cause a variety of gastrointestinal diseases, including non-symptomatic chronic gastritis, peptic ulcers, gastric adenocarcinoma, and gastric MALT lymphoma [17-19]. The molecular mechanisms underlying these diseases are also beginning to be elucidated from both the standpoint of the host and bacteria, but few studies have evaluated the metabolite alterations induced in the host by *H. pylori* infections using metabolomic analysis. In our previous study, C57BL/6J mice were infected with the *H. pylori* SS1 strain, and then the alterations in the levels of metabolites that occurred in the stomachs of the infected mice were assessed. Consequently, it was found that some metabolite pathways were altered by *H. pylori* in an infection period-dependent manner [20]. At 1 month after the start of the *H. pylori* SS1 infection, the glycolytic pathway, the TCA cycle, and the choline pathway tended to be upregulated. At 6 months post-infection, the urea cycle tended to be downregulated. In the stomach tissue of the *H. pylori* SS1-infected mice, high levels of some amino acids were observed at 1 month post-infection, and low levels of many amino acids were detected at 3 and 6 months post-infection. However, the extent of these alterations was relatively small, which might have been due to the diversity of the cells found in the stomach, as information derived from a variety of cell types might be affected by “cancelling out” effects. Therefore, in this study *in vitro* infection experiments using

AGS human gastric carcinoma cells were performed with the aim of obtaining novel insights into *H. pylori* infections via metabolomics. Specifically, we investigated whether *H. pylori* causes metabolic abnormalities in gastric epithelial cells.

In AGS cells that had been infected with *H. pylori*, characteristic alterations in amino acid levels were observed (**Table S1**, **Fig. S2**). At 2 hour post-infection, the levels of many amino acids tended to be lower in the *H. pylori*-infected AGS cells than in the uninfected AGS cells. On the contrary, at 6 and 12 hour post-infection, the opposite tendency was noted. These results suggest the following possibility: In the gastric epithelial cells infected with *H. pylori*, a variety of biological responses are induced, and then the amino-acid availability is enhanced in response to the *H. pylori* infection. Reduced levels of amino acids could trigger processes that increase the amino acid supply, resulting in increased levels of some amino acids. These increases in the levels of some amino acids might be caused by protein degradation. Previously, it was reported that autophagy was induced in AGS cells that had been infected with *H. pylori* [21]. On the contrary, the activity levels of three major proteasomes; i.e., chymotrypsin-like activity, peptidylglutamyl peptide-hydrolyzing-like activity, and trypsin-like activity, were decreased in AGS cells cultured with *H. pylori* [22]. In another study, the ubiquitin-proteasome pathway was activated in *H. pylori*-infected AGS cells [23], and *H. pylori* also activated calpain in MKN45 cells [24]. As shown in these studies, *H. pylori* infections may affect protein degradation, and our results suggest that protein degradation might be enhanced by *H. pylori*, because the levels of many amino acids were increased at 6 and 12 hour post-infection (**Table S1**). In our study, MG132, which is an inhibitor of proteasomes and calpains, inhibited the *H.*

pylori-induced upregulation of TNF- α and IL-8 mRNA expression (**Fig. 3**). MG132 is known to regulate the expression of pro-inflammatory cytokines and their receptors via the inhibition of nuclear factor- κ B activation [25]. In addition, in our study, it was examined how MG132 affects the metabolite profile in AGS cells (**Table S2**), because we considered that the MG132 treatment inhibits the degradation of some proteins resulting in the decreased levels of amino acids in AGS cells. However, unlike expectations, regarding the metabolites evaluated in **Fig. S2**, most of the targeted metabolites were increased by the MG132 treatment in the uninfected AGS cells. These results were not limited to the presence or absence of *H. pylori* infection, and the similar results were observed in *H. pylori*-infected AGS cells. (**Table S2**). These results mean that the *H. pylori*-induced increases in the levels of amino acids were not cancelled by the MG132 treatment, and also indicate that the inhibition of protein degradation seems to increase the levels of many amino acids in the cells rather than suppressing the increased levels of amino acids. When the MG132-treated AGS cells were infected with *H. pylori*, the *H. pylori*-caused inflammatory responses were suppressed (**Fig. 3**), and the levels of many amino acids were increased under this environment (**Table S2**). On the contrary, the *H. pylori* infection also induced the increased levels of amino acids (**Table S1**), and the *H. pylori* infection caused inflammatory responses. Therefore, the increased levels of amino acids may not be much associated with the inflammatory responses the *H. pylori* infection. MG132 is known to inhibit the cell growth at its lower concentration [26], and the inhibited cell growth may induce the increases in the levels of amino acids in the cells. Therefore, the further investigations of the relationship between amino acid alterations and biological responses to *H. pylori* infections are necessary.

The increased levels of amino acids might be deeply involved in host responses to *H. pylori* infections, although we could not clarify whether these stimuli caused the increased levels of amino acids via the declined availability of amino acids or the enhanced supply of amino acids from proteins and others. Interestingly, the concentration of asparagine in AGS cells was reduced by the infection with *H. pylori*. Asparagine is generated from L-aspartic acid by ASNS (**Fig. S3**). Therefore, we considered that the reduced level of asparagine seen in the *H. pylori*-infected AGS cells might have been caused by the inactivation of ASNS, possibly leading to affecting the biological responses to the *H. pylori* infection. As a result, the level of ASNS tended to be increased in the *H. pylori*-infected AGS cells compared with the non-infected AGS cells without the significant difference ($p=0.069$) (**Fig. 2**). On the other hand, the ASNS downregulation suppressed the *H. pylori*-induced IL-8 upregulation in AGS cells (**Fig. 2**). In the case of depletion of asparagine in the cells, asparagine should be generated to maintain homeostasis. Therefore, we created an environment with the lower level of asparagine based on the ASNS downregulation that cannot produce asparagine in the cells (**Fig. 2**). In this environment, the *H. pylori*-induced IL-8 upregulation was significantly inhibited. Therefore, these results suggest as follows: Asparagine is used in the AGS cells after the infection with *H. pylori*. This usage of asparagine may be related to the host inflammatory responses to the *H. pylori* infection. This enhancement of asparagine availability in the *H. pylori*-infected AGS cells may be also explained by the significantly decreased level of asparagine at as little as 2 hours after the *H. pylori* infection as well as 6 and 12 hours. In a study by Yu et al., it was reported that transient knockdown of ASNS inhibited cell proliferation and tumor growth in human gastric AGS and MKN45 cells, and moreover the low expression of ASNS was significantly

associated with better survival in gastric cancer patients [27]. Asparaginase also changes asparagine into aspartic acid, so the lower level of asparagine might be also explained by the upregulation of asparaginase activity in the *H. pylori*-infected AGS cells. Asparagine enhances the proliferation of cancer cells [28], and therefore, asparaginase has been used as an anti-cancer drug. In addition, *H. pylori* also possesses its own asparaginase, and it was suggested that *H. pylori* asparaginase is a novel antigen that functions as a cell-cycle inhibitor of fibroblasts and gastric cells [29]. Therefore, *H. pylori* asparaginase might have contributed to the reduction in the level of asparagine seen in the *H. pylori*-infected AGS cells. Taken together, previous reports and our results suggest that the declined level of asparagine in AGS cells infected with *H. pylori* expresses the biological responses to the *H. pylori* infection. Possibly, AGS cells infected with *H. pylori* effectively may utilize asparagine, leading to cell proliferation, tumor growth, and inflammatory responses.

H. pylori also affected the regulation of the TCA cycle. The TCA cycle is a set of important biological reactions based on aerobic metabolism and produces energy efficiently through the oxidation of acetyl-coenzyme A (CoA) into CO₂ and the production of ATP as a form of chemical energy. In addition, the TCA cycle supplies biosynthetic precursors, such as amino acids and NADH. At 2 hour post-infection, a tendency towards the downregulation of the TCA cycle was observed, whereas the TCA cycle tended to be upregulated at 6 and 12 hour post-infection, although the latter half of the TCA cycle was not so much changed (**Table S1**). These changes seemed to be linked to alterations in amino acid levels, which is reasonable because amino acids are also available as nutrients. Regarding the TCA cycle, marked increases in the levels of citric

acid and isocitric acid were observed in the AGS cells that had been infected with *H. pylori* for 6 or 12 hours (**Table S1**). Interestingly, the increased levels of citric acid and isocitric acid were also observed in the MG132-treated AGS cells. However, in the case of the *H. pylori* infection, the downstream, for example fumaric acid and malic acid, was not much increased (**Table S1**). On the other hand, the downstream was upregulated by the MG132 treatment (**Table S2**). This difference is interesting, and probably due to regulation of IDHs by the *H. pylori* infection (**Fig. 4**). Citric acid and isocitric acid are intermediates in the TCA cycle, and citric acid is converted into isocitric acid via aconitic acid. Usually, citric acid is used as an intermediate in the TCA cycle. However, citrate can also be transferred out of mitochondria so that it can be used to synthesize fatty acids. Whether citric acid is used for the TCA cycle or for fatty acid synthesis is regulated by IDHs. In this study, *H. pylori* reduced the enzymatic activity of IDH in AGS cells (**Fig. 4**). Therefore, fatty acid biosynthesis might be upregulated in AGS cells during *H. pylori* infections. Fatty acids have multiple biological functions, and enhanced fatty acid synthesis might be involved in the biological responses of AGS cells to *H. pylori* infections. Actually, it was reported that citric acid can activate the enzymatic activity of acetyl CoA carboxylase, leading to greater synthesis of fatty acids [30]. Citric acid can also induce apoptotic cell death via the mitochondrial pathway in human gastric carcinoma cell lines [31]. Taken together, the *H. pylori*-induced marked increases in the levels of citric acid and isocitric acid seen in the current study might be closely related to the biological responses of gastric epithelial cells to *H. pylori* infections.

This study had some limitations. There are various strains of *H. pylori*, which possess a

broad range of virulence factors, for example CagA. In addition, this broad range of virulence factors seems to contribute to the variety of *H. pylori*-related gastric diseases. The *H. pylori* strain (ATCC43504) used in this study had Western-type CagA and sla-m1-type VacA virulence factors. To elucidate the detailed relationships among *H. pylori* infection and metabolite alterations in gastric epithelial cells, and furthermore, to understand the involvement of metabolite alterations in *H. pylori*-related gastric diseases, for example, the *cagA* positive *H. pylori* strain and its isogenic *cagA*-deficient strain needed to be constructed for the comparative trials. In addition, Western-type and East Asian-type CagA positive *H. pylori* strains should be compared by using isogenic mutant strains. In the future, comparative trials involving a variety of *H. pylori* strains should be carried out. Moreover, AGS cells that are one of gastric epithelial cell lines derived from a patient with gastric adenocarcinoma were used in this study, and this is an important consideration, because the metabolome in AGS cells that are the transformed cells isolated from cancer may not mimic normal gastric epithelial cells. The *H. pylori*-infected AGS cells may mimic normal gastric epithelial cells that are exposed to *H. pylori*, because AGS cells have been widely applied to the experiments about the response to *H. pylori*. This should be considered as the limitations to this study when interpreting the results from our study. Our study showed that the infection of gastric epithelial cells with *H. pylori* alters metabolic pathways, and furthermore these alterations may affect the biological responses to the *H. pylori* infection. This is the first trial to involve *in vitro* experiments with cultured cells. Our findings are important for increasing current understanding of *H. pylori*-related gastric diseases.

Funding:

This study was supported by a Grant-in-Aid for Scientific Research (B) from the Japan Society for the Promotion of Science (16H05227) [M.Y.], the AMED-CREST by the Japan Agency for Medical Research and Development (17gm0710013h0004) [S.N. and M.Y.], and a grant from the Hyogo Science and Technology Association [S.N.].

Acknowledgements:

We appreciate very much the technical support and the meaningful advices from Takeshi Azuma (Kobe University Graduate School of Medicine).

Conflict of interest:

The authors declare that they have no conflict of interest.

References

1. B.J. Marshall, J.R. Warren, Unidentified curved bacilli in the stomach of patients with gastritis and peptic ulceration. *Lancet* 1(1984) 1311-1315.
2. IARC: Monographs on the Evaluation of Carcinogenic risks to Human. <http://monographs.iarc.fr/>
3. T. Kwok, S. Backert, H. Schwarz, J. Berger, T.F. Meyer, Specific entry of *Helicobacter pylori* into cultured gastric epithelial cells via a zipper-like mechanism. *Infect. Immun.* 70 (2002) 2108-2120.
4. E. Goni, F. Franceschi, *Helicobacter pylori* and extragastric diseases. *Helicobacter* 21 (2016) 45-48.
5. L.J. van Doorn, C. Figueiredo, R. Sanna, A. Plaisier, P. Schneeberger, de W. Boer, W. Quint, Clinical relevance of the *cagA*, *vacA*, and *iceA* status of *Helicobacter pylori*. *Gastroenterology* 115 (1998) 58-66.
6. S. Backert, N. Tegtmeyer, M. Selbach, The versatility of *Helicobacter pylori* CagA effector protein functions: The master key hypothesis. *Helicobacter* 15 (2010) 163-176.
7. M. Hatakeyama, Anthropological and clinical implications for the structural diversity of the *Helicobacter pylori* CagA oncoprotein. *Cancer Sci.* 102 (2011) 36-43.
8. A. Tohidpour, CagA-mediated pathogenesis of *Helicobacter pylori*. *Microb. Pathog.* 93 (2016) 44-55.
9. M. Boncristiano, S.R. Paccani, S. Barone, C. Ulivieri, L. Patrussi, D. Ilver, A. Amedei, M.M. D'Elis, J.L. Telford, C.T. Baldari, The *Helicobacter pylori* vacuolating toxin inhibits T cell activation by two independent mechanisms. *J. Exp.*

525 Med. 198 (2003) 1887-1897.

526 **10.** S. Backert, H. Gressmann, T. Kwok, U. Zimny-Arndt, W. König, P.R. Jungblut, T.F.
527 Meyer, Gene expression and protein profiling of AGS gastric epithelial cells upon
528 infection with *Helicobacter pylori*. Proteomics 5 (2005) 3902-3918.

529 **11.** C. Holland, M. Schmid, U. Zimny-Arndt, J. Rohloff, R. Stein, P.R. Jungblut, T.F.
530 Meyer, Quantitative phosphoproteomics reveals link between *Helicobacter pylori*
531 infection and RNA splicing modulation in host cells. Proteomics 11 (2011)
532 2798-2811.

533 **12.** M. Yoshida, N. Hatano, S. Nishiumi, Y. Irino, Y. Izumi, T. Takenawa, T. Azuma,
534 Diagnosis of gastroenterological diseases by metabolome analysis using gas
535 chromatography-mass spectrometry. J. Gastroenterol. 47 (2012) 9-20.

536 **13.** T. Yoshie, S. Nishiumi, Y. Izumi, A. Sakai, J. Inoue, T. Azuma, M. Yoshida,
537 Regulation of the metabolite profile by an APC gene mutation in colorectal cancer.
538 Cancer. Sci. 103 (2012) 1010-1021.

539 **14.** H. Tsugawa, T. Bamba, M. Shinohara, S. Nishiumi, M. Yoshida, E. Fukusaki,
540 Practical Non-targeted Gas Chromatography/Mass Spectrometry-based
541 Metabolomics Platform for Metabolic Phenotype Analysis. J. Biosci. Bioeng. 112
542 (2011) 292-298.

543 **15.** H. Tanaka, M. Yoshida, S. Nishiumi, N. Ohnishi, K. Kobayashi, K. Yamamoto, T.
544 Fujita, M. Hatakeyama, T. Azuma, The CagA protein of *Helicobacter pylori*
545 suppresses the functions of dendritic cell in mice. Arch. Biochem. Biophys. 498
546 (2010) 35-42.

547 **16.** X.M. Fan, B.C. Wong, W.P. Wang, X.M. Zhou, C.H. Cho, S.T. Yuen, S.Y. Leung,
548 M.C. Lin, H.F. Kung, S.K. Lam, Inhibition of proteasome function induced

apoptosis in gastric cancer. Int. J. Cancer. 93 (2001) 481-488.

17. A. Morgner, E. Bayerdörffer, A. Neubauer, M. Stolte, Malignant tumors of the stomach. Gastric mucosa-associated lymphoid tissue lymphoma and *Helicobacter pylori*, Gastroenterol. Clin. North Am. 29 (2000) 593-607.

18. P.G. Isaacson, Recent developments in our understanding of gastric lymphomas, Am. J. Surg. Pathol. 20 (1996) 1-7.

19. S.J. Veldhuyzen van Zanten, P.M. Sherman, *Helicobacter pylori* infection as a cause of gastritis, duodenal ulcer, gastric cancer and nonulcer dyspepsia: a systemic overview. CMAJ 150 (1994) 177-185.

20. S. Nishiumi, M. Yoshida, T. Azuma, Alterations in metabolic pathways in stomach of mice infected with *Helicobacter pylori*. Microb. Pathog. 109 (2017) 78-85.

21. M.R. Terebiznik, D. Raju, C.L. Vázquez, K. Torbricki, R. Kulkarni, S.R. Blanke, T. Yoshimori, M.I. Colombo, N.L. Jones, Effect of *Helicobacter pylori*'s vacuolating cytotoxin on the autophagy pathway in gastric epithelial cells. Autophagy. 5 (2009) 370-379.

22. H. Eguchi, N. Herschenhous, N. Kuzushita, S.F. Moss, *Helicobacter pylori* increases proteasome-mediated degradation of p27(kip1) in gastric epithelial cells. Cancer Res. 63 (2003) 4739-4746.

23. X. Tang, S. Wen, D. Zheng, L. Tucker, L. Cao, D. Pantazatos, S.F. Moss, B. Ramratnam, Acetylation of drosha on the N-terminus inhibits its degradation by ubiquitination. PLoS One. 8 (2013) e72503.

24. P.M. O'Connor, T.K. Lapointe, S. Jackson, P.L. Beck, N.L. Jones, A.G. Buret, *Helicobacter pylori* activates calpain via toll-like receptor 2 to disrupt adherens junctions in human gastric epithelial cells. Infect. Immun. 79 (2011) 3887-3894.

- 573 **25.** P.C. Ortiz-Lazareno, G. Hernandez-Flores, J.R. Dominguez-Rodriguez, J.M.
574 Lerma-Diaz, L.F. Jave-Suarez, A. Aguilar-Lemarroy, P.C. Gomez-Contreras, D.
575 Scott-Algara, A. Bravo-Cuellar, MG132 proteasome inhibitor modulates
576 proinflammatory cytokines production and expression of their receptors in U937
577 cells: involvement of nuclear factor- κ B and activator protein-1. *Immunology* 124
578 (2008) 534-541.
- 579 **26.** M. Vivier, M. Rapp, J. Papon, P. Labarre, M.J. Galmier, J. Sauzière, J.C.
580 Madelmont, Synthesis, radiosynthesis, and biological evaluation of new proteasome
581 inhibitors in a tumor targeting approach. *J. Med. Chem.* 51 (2008) 1043-1047.
- 582 **27.** Q. Yu, X. Wang, L. Wang, J. Zheng, J. Wang, B. Wang, Knockdown of asparagine
583 synthetase (ASNS) suppresses cell proliferation and inhibits tumor growth in
584 gastric cancer cells. *Scand. J. Gastroenterol.* 51 (2016) 1220-1226.
- 585 **28.** A.S. Krall, S. Xu, T.G. Graeber, D. Braas, H.R. Christofk, Asparagine promotes
586 cancer cell proliferation through use as an amino acid exchange factor. *Nat.*
587 *Commun.* 7 (2016) 11457.
- 588 **29.** C. Scotti, P. Sommi, M.V. Pasquetto, D. Cappelletti, S. Stivala, P. Mignosi, M.
589 Savio, L.R. Chiarelli, G. Valentini, V.M. Bolanos-Garcia, D.S. Merrell, S. Franchini,
590 M.L. Verona, C. Bolis, E. Solcia, R. Manca, D. Franciotta, A. Casasco, P. Filipazzi,
591 E. Zardini, V. Vannini, Cell-cycle inhibition by *Helicobacter pylori* L-asparaginase.
592 *PLoS One* 5 (2010) e13892.
- 593 **30.** P.R. Vagelos, A.W. Alberts, D.B. Martin, Studies on the mechanism of activation of
594 acetyl coenzyme A carboxylase by citrate. *J. Biol. Chem.* 138 (1963) 533-540.
- 595 **31.** Y. Lu, X. Zhang, H. Zhang, J. Lan, G. Huang, E. Varin, H. Lincet, L. Poulain, P.
596 Icard, Citrate induces apoptotic cell death: a promising way to treat gastric

597 carcinoma? Anticancer Res. 31 (2011) 797-805.

598

599

Figure legends

Fig. 1. The morphological appearance of *H. pylori*-infected AGS cells

(A) AGS cells were infected with *H. pylori* (ATCC43504) for 6 or 12 hours, and then the morphological appearance of the AGS cells was examined. Typical images are shown in **Fig. 1(A)**. (B) AGS cells were infected with *H. pylori* (ATCC43504) for 5 hours, and then CagA and phosphorylated CagA in AGS cells was examined by Western blotting. Typical images are shown in **Fig. 1(B)**. IB: Immunoblot; IP: Immunoprecipitation.

Fig. 2. The effects of ASNS downregulation on IL-8 mRNA expression in *H. pylori*-infected AGS cells

(A) To confirm the downregulation of ASNS by siRNA, AGS cells were treated with 100, 200 or 500 pmols ASNS siRNA (#1 and #2) or the control siRNA as a vehicle control for 48 hours, and then proteins in AGS cells were extracted. The proteins were subjected to Western blotting, and ASNS and β -actin were detected. (B) To downregulate ASNS expression, AGS cells were treated with 100 pmols ASNS siRNA (#1 and #2) or the control siRNA as a vehicle control for 48 hours. AGS cells were infected with *H. pylori* (ATCC43504) for the last 18 hours of 48 hours. RNA was extracted from the cells, and then ASNS and IL-8 mRNA expressions were evaluated via the real-time PCR. Data are shown as the mean \pm SEM (n=3), and asterisks indicate significant differences between each group.

Fig. 3. The effects of proteasome and calpain inhibition on TNF- α and IL-8 mRNA expression *H. pylori*-infected AGS cells

AGS cells were pre-incubated with 0.5 μ M MG132 or DMSO as a vehicle control for 30 minutes and then were infected with *H. pylori* (ATCC43504) for 12 hours. RNA was extracted from the cells, and then the mRNA expression levels of TNF- α and IL-8 were evaluated using the real-time PCR. Data are shown as the mean \pm SEM (n=3), and different letters indicate significant differences.

Fig. 4. The effects of *H. pylori* infection on IDH mRNA expression and IDH activity in AGS cells

AGS cells were infected with *H. pylori* (ATCC43504) for 6 or 12 hours. (A) Then, RNA was extracted from the cells, and the mRNA expression levels of IDH1, IDH2, and IDH3a were evaluated using the real-time PCR. Data are shown as the mean \pm SEM (n=3). (B) AGS cells that had been infected with *H. pylori* (ATCC43504) for 6 or 12 hours also had their NAD⁺-dependent IDH and NADP⁺-dependent IDH activity measured. Data are shown as the mean \pm SEM (n=4), and asterisks indicate significant differences between each group.

Figure 1

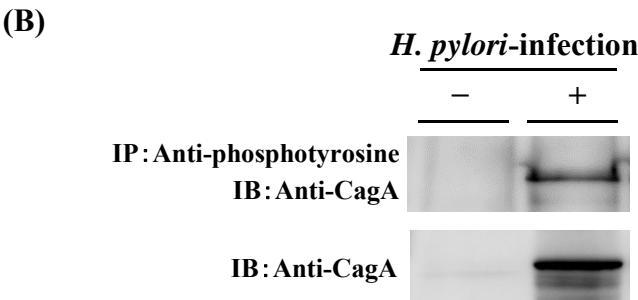
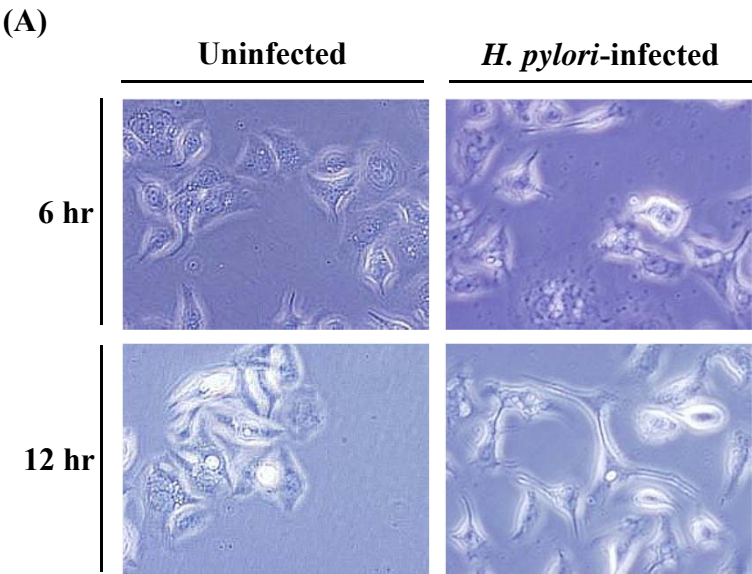


Figure 2

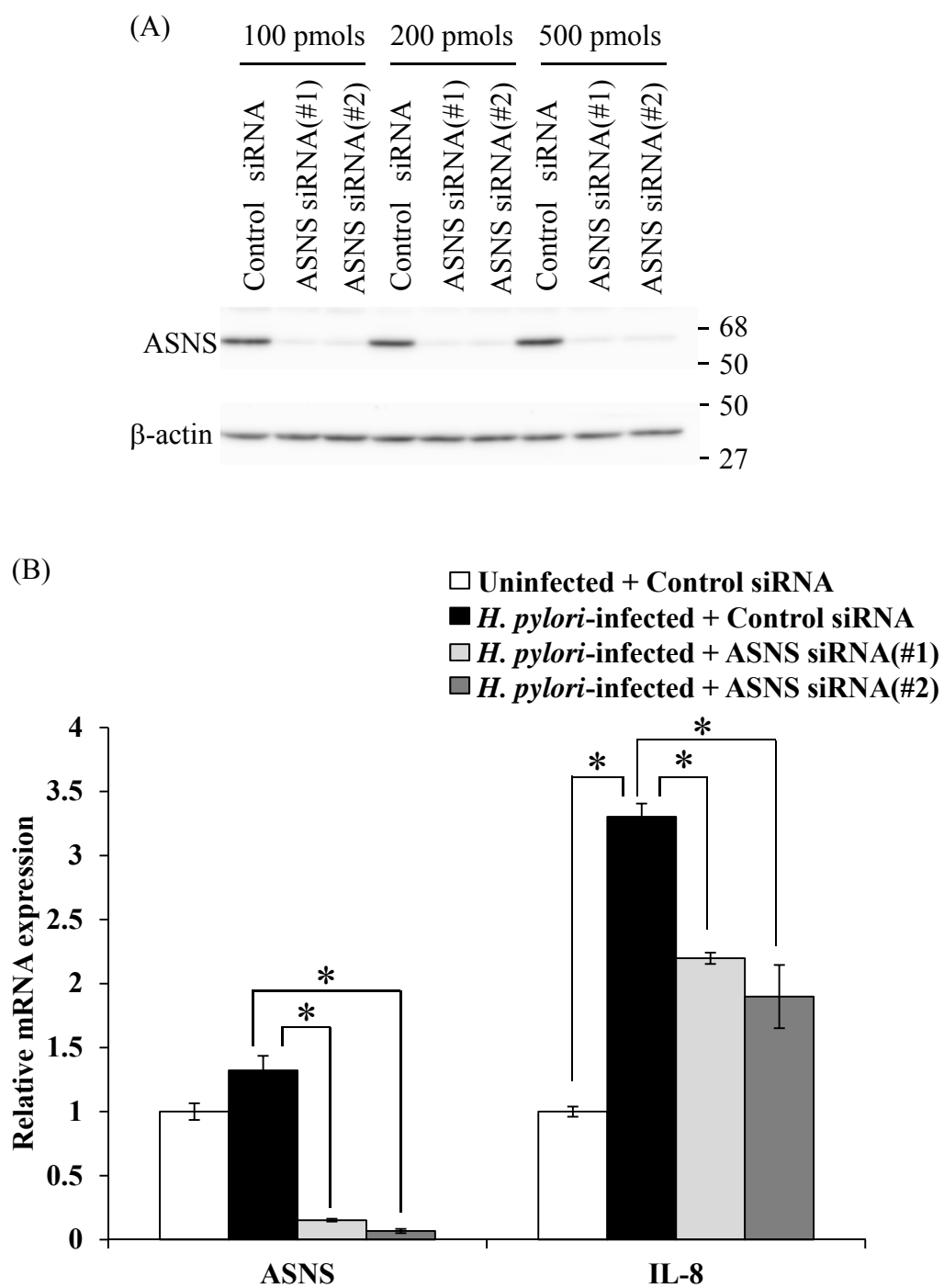


Figure 3

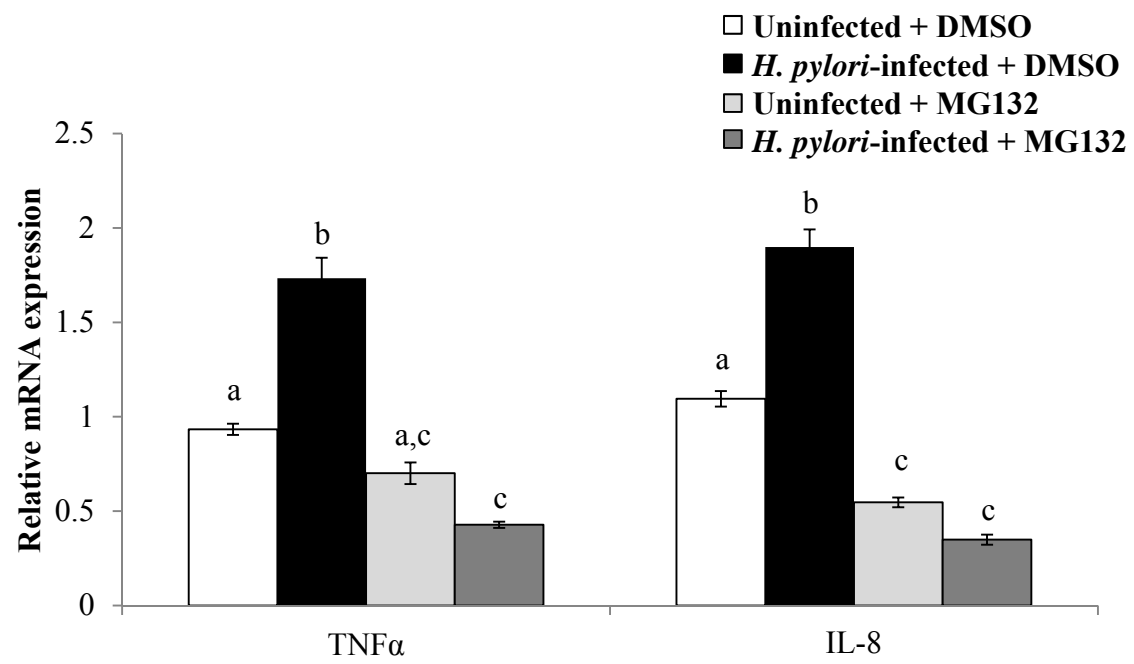


Figure 4

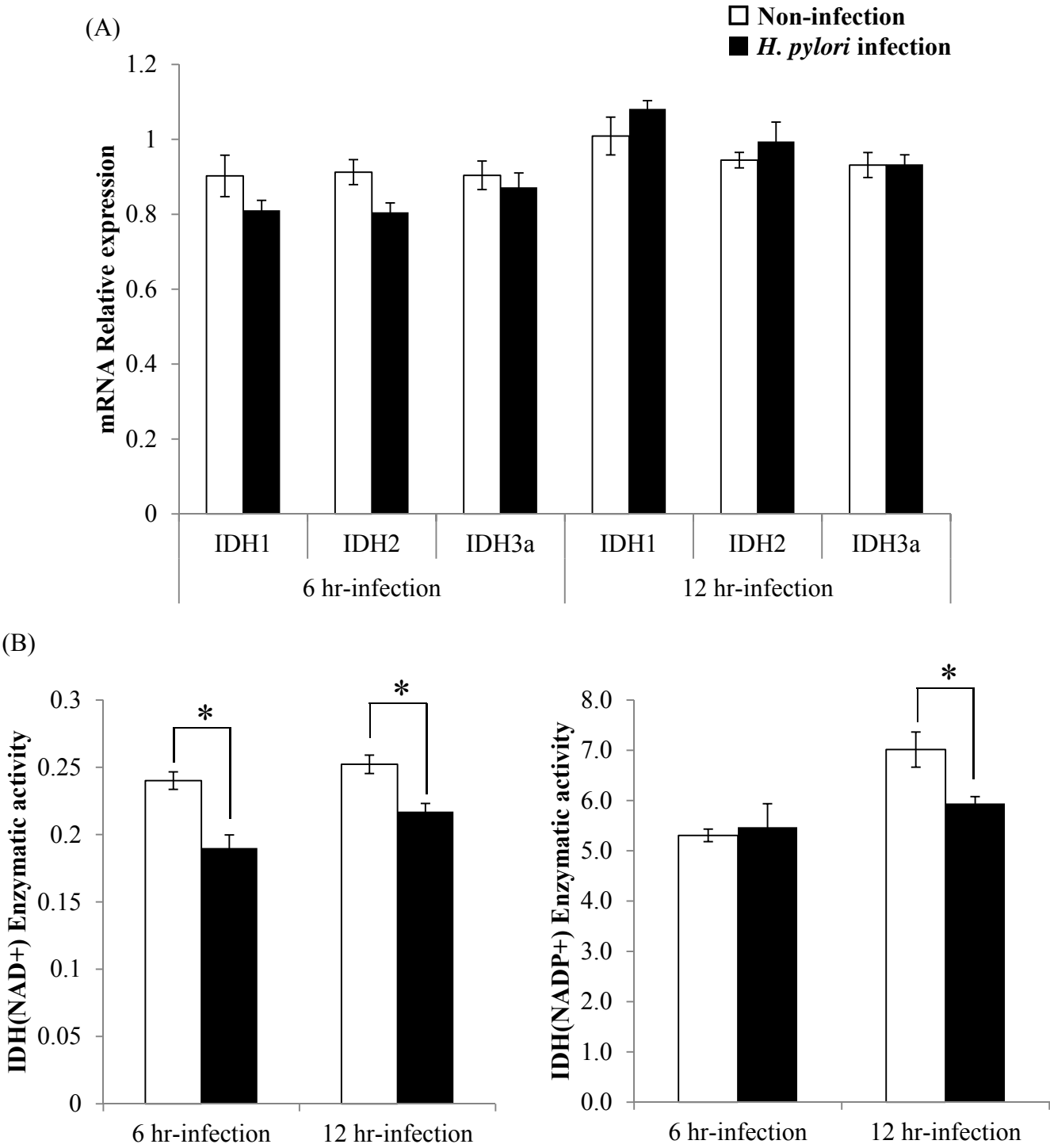


Table S1. Metabolite profiles of *H. pylori* i-infected AGS cells at 2, 6, and 12 hr post-infection

Compound name	2 hr post-infection		6 hr post-infection		12 hr post-infection	
	Fold induction	P-value	Fold induction	P-value	Fold induction	P-value
	<i>H. pylori</i> -infected/uninfected		<i>H. pylori</i> -infected/uninfected		<i>H. pylori</i> -infected/uninfected	
Acetoacetic acid	0.95	0.58	1.23	0.48	1.30	0.19
N-acetyl-D-glucosamine 2	1.02	0.91	1.32	0.29	0.81	0.47
N- α -acetyl-L-lysine 2	1.14	0.52	0.98	0.94	1.65	0.05
N-acetyl-DL-valine	0.96	0.90	0.83	0.52	1.40	0.23
Adenine	1.04	0.86	1.10	0.75	1.07	0.82
Alanine (2TMS)	0.96	0.79	1.14	0.31	1.25	0.25
β -alanine	0.89	0.31	1.01	0.97	1.06	0.79
2-aminoethanol	0.93	0.56	1.92	0.25	1.32	0.04^a
2-aminoisobutyrate	0.94	0.61	1.31	0.54	0.96	0.88
2-aminopimelic acid	1.23	0.46	1.54	0.01^a	2.28	0.06
5-aminovaleric acid	0.42	0.18	0.98	0.96	2.35	0.06
1,6-anhydroglucose	0.76	0.36	0.52	0.01^a	1.01	0.94
Asparagine	0.72	0.01^a	0.66	0.04^a	0.73	0.39
Aspartic acid	0.93	0.61	1.23	0.32	1.19	0.42
Citric acid + Isocitric acid	0.96	0.8	1.52	0.01^a	2.42	0.02^a
Cysteine + Cystine	1.11	0.63	1.52	0.25	0.81	0.36
Cysteine sulfonic acid	1.03	0.81	0.98	0.92	1.09	0.74
2-dehydro-D-gluconate 1	1.09	0.37	1.21	0.40	1.04	0.81
2'-deoxyribose-5'-phosphate	0.82	0.15	1.14	0.66	0.87	0.58
Dopa	0.91	0.41	0.81	0.54	0.70	0.44
Fumaric acid	0.88	0.57	1.24	0.17	1.11	0.45
Galactosamine 1	1.04	0.88	0.95	0.87	1.22	0.25
Glucose 1	1.08	0.80	1.01	0.94	1.01	0.88
Glutamic acid	0.88	0.39	1.06	0.68	1.04	0.87
Glutamine	0.74	0.30	0.90	0.79	1.10	0.79
Glyceric acid	0.96	0.80	1.43	0.40	1.58	0.06
Glycerol	0.89	0.33	0.82	0.10	1.01	0.92
Glycine (3TMS)	0.96	0.71	1.29	0.12	1.49	0.03^a
1-hexadecanol	0.89	0.68	1.23	0.48	1.10	0.74
Homocysteine 1	0.99	0.91	1.12	0.62	0.84	0.57
Homoserine	0.96	0.93	1.02	0.96	1.13	0.81
trans-4-hydroxy-L-proline	0.99	0.95	1.18	0.26	1.48	0.17
Hypoxanthine	0.82	0.08	1.22	0.44	2.35	0.08
Indole-3-acetaldehyde 2	1.02	0.91	1.32	0.29	0.89	0.57
Inositol	0.92	0.32	0.93	0.49	1.02	0.88
Isoleucine	1.09	0.53	1.26	0.06	1.29	0.06
Ketovaline 2	1.06	0.71	1.36	0.18	1.09	0.61
Lactic acid	0.93	0.42	1.23	0.31	1.15	0.17
Lauric acid	0.77	0.20	0.57	0.08	0.85	0.49
Malic acid	0.96	0.83	1.26	0.04^a	1.22	0.19
Methionine	1.32	0.44	1.46	0.25	0.97	0.93
Nicotinamide	1.02	0.90	1.07	0.66	0.99	0.93
Nonanoic acid (C9)	1.02	0.86	1.03	0.86	0.95	0.71
Norleucine (1TMS)	0.95	0.86	0.78	0.64	0.95	0.88
Ornithine	0.97	0.82	1.03	0.86	1.15	0.67
Oxalate	1.17	0.46	1.25	0.21	1.07	0.65
Oxaloacetic acid + Pyruvate	0.98	0.89	1.18	0.41	1.26	0.15
Phenylalanine	1.00	0.99	1.26	0.10	1.36	0.09
α -phenylglycine	1.40	0.19	1.28	0.17	1.83	0.09
Phosphate	0.90	0.33	0.82	0.11	0.98	0.85
Phosphoenolpyruvic acid	0.83	0.09	1.28	0.16	0.94	0.68
O-phosphoethanolamine	0.76	0.47	1.00	0.99	1.70	0.05
2,3-bisphospho-glycerate	1.13	0.52	0.94	0.62	1.01	0.91
Prolinamide	0.93	0.70	0.94	0.84	1.33	0.56
Proline	0.93	0.70	1.06	0.77	1.07	0.70
Ribitol	0.76	0.38	1.33	0.32	1.35	0.10
Ribose	1.09	0.37	1.24	0.53	1.70	0.05
Ribulose-5-phosphate 2	0.84	0.06	1.20	0.43	1.52	0.18
Serine (3TMS)	1.13	0.37	1.22	0.08	1.60	0.01^a
α -sorbopyranose 1 (or fructose 1)	1.04	0.89	1.24	0.47	0.96	0.75
Succinic acid (or aldehyde)	0.92	0.18	1.04	0.60	1.06	0.44
Taurine	0.97	0.94	0.97	0.94	1.38	0.02^a
Threonine (3TMS)	1.03	0.83	1.23	0.07	1.46	0.03^a
Tryptophan	0.97	0.78	1.15	0.32	1.31	0.11
Tyrosine	0.96	0.70	1.12	0.25	1.30	0.05
Uracil	1.26	0.50	1.52	0.30	1.18	0.25
Valine (2TMS)	1.03	0.78	1.34	0.04^a	1.37	<0.01^a

AGS cells were serum-starved for 16 hr, and the cells were harvested at 2, 6, or 12 hr after being infected. Data are represented as fold-induction values of the normalized peak intensity for the *H. pylori*-infected AGS cells (n=5) versus that of the uninfected controls (n=5). P-values for comparisons between the *H. pylori*-infected AGS cells and the corresponding control cells were calculated using the Student's t-test in each infection period, and superscript letters (a) indicate P-values of <0.05.

Table S2. The effects of MG132 on the metabolite profiles in the *H. pylori*-infected and uninfected AGS cells

Compound name	Fold induction	P-value	Fold induction	P-value
	MG132/DMSO		MG132 + <i>H. pylori</i> infection /DMSO + <i>H. pylori</i> infection	
Alanine (2TMS)	1.83	0.064	2.25	0.003^a
β-Alanine	1.73	0.141	1.85	0.047^a
Asparagine	2.04	0.010^a	3.04	0.018^a
Aspartic acid	2.74	0.012^a	2.80	0.023^a
Citric acid + Isocitric acid	3.35	0.011^a	3.54	0.026^a
Cysteine+Cystine	4.12	0.003^a	4.27	0.019^a
Fumaric acid	3.11	0.022^a	3.10	0.017^a
Glucose_1	1.44	0.207	1.49	0.090
Glutamic acid	1.67	0.159	2.09	0.224
Glutamine	2.79	<0.001^a	4.41	0.015^a
Glyceric acid	2.42	<0.001^a	2.32	0.035^a
Glycine (3TMS)	4.92	<0.001^a	2.55	0.026^a
trans-4-Hydroxy-L-proline	5.99	0.030^a	5.36	0.002^a
Isoleucine	2.13	0.031^a	3.86	0.019^a
Lactic acid	2.61	<0.001^a	2.56	0.014^a
Malic acid	4.04	0.011^a	2.58	0.026^a
Methionine	4.17	0.003^a	4.17	0.007^a
Ornithine	1.40	0.311	0.90	0.819
Oxalacetic acid + Pyruvate	2.22	0.016^a	2.18	0.026^a
Phenylalanine	2.41	0.030^a	3.19	0.005^a
Phosphoenolpyruvic acid	3.62	0.013^a	5.59	0.014^a
Proline	2.63	0.042^a	2.84	0.003^a
Serine (3TMS)	0.91	0.435	0.86	0.523
Succinic acid (or aldehyde)	2.20	0.045^a	1.52	0.100
Threonine (3TMS)	1.14	0.752	1.13	0.672
Tryptophan	2.47	0.002^a	3.35	0.017^a
Tyrosine	3.41	0.006^a	4.30	0.032^a
Valine (2TMS)	1.81	0.061	2.21	0.141

AGS cells were serum-starved for 16 hr, and then the cells were pre-incubated with 0.5 mM MG132 dissolved in dimethyl sulfoxide (DMSO) for 30 min, before being infected with *H. pylori* for 12 hr. The results of the metabolites evaluated in Supporting Figure 1 are listed in Supporting Table 2, but taurine is not included in Supporting Table 2, because it could not be detected in the MG132-treated AGS cells. Data are represented as fold-induction values of the normalized peak intensity for the MG132-treated AGS cells (n=4) versus that of the non-treated AGS cells (n=4) or the MG132-treated & *H. pylori*-infected AGS cells (n=4) versus the DMSO-treated & *H. pylori*-infected AGS cells (n=4). P-values for comparisons between each 2 group were calculated using the Student's t-test, and superscript letters (a) indicate P-values of <0.05.

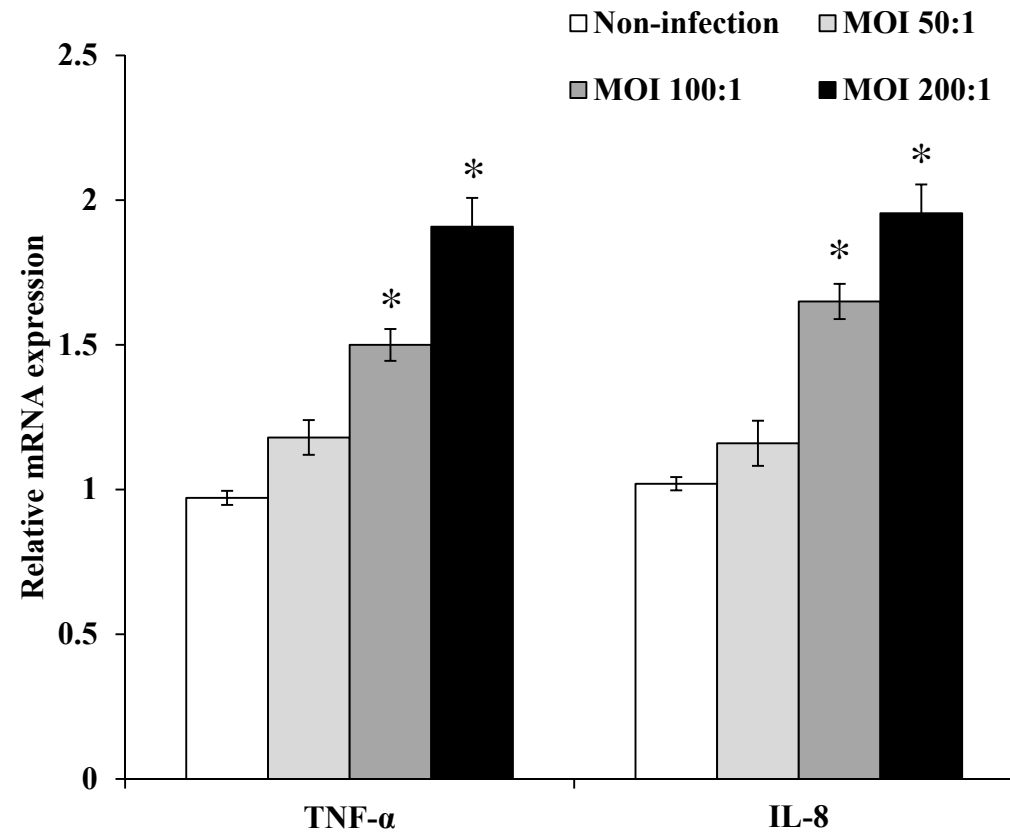


Figure S1. TNF- α and IL-8 mRNA expressions in the AGS cells infected with *H. pylori* strain ATCC43504

AGS cells were infected with *H. pylori* (ATCC43504) at MOI of 50:1, 100:1 or 200:1 for 12 hours, and then were subjected to evaluations of TNF- α and IL-8 mRNA expressions. Data are shown as the mean \pm SEM (n=3). Asterisks indicate significant differences ($P < 0.05$) between the *H. pylori*-infected AGS cells and uninfected controls. The Student's t-test was used for comparisons between the two groups.

(2-hour *H. pylori* infection)

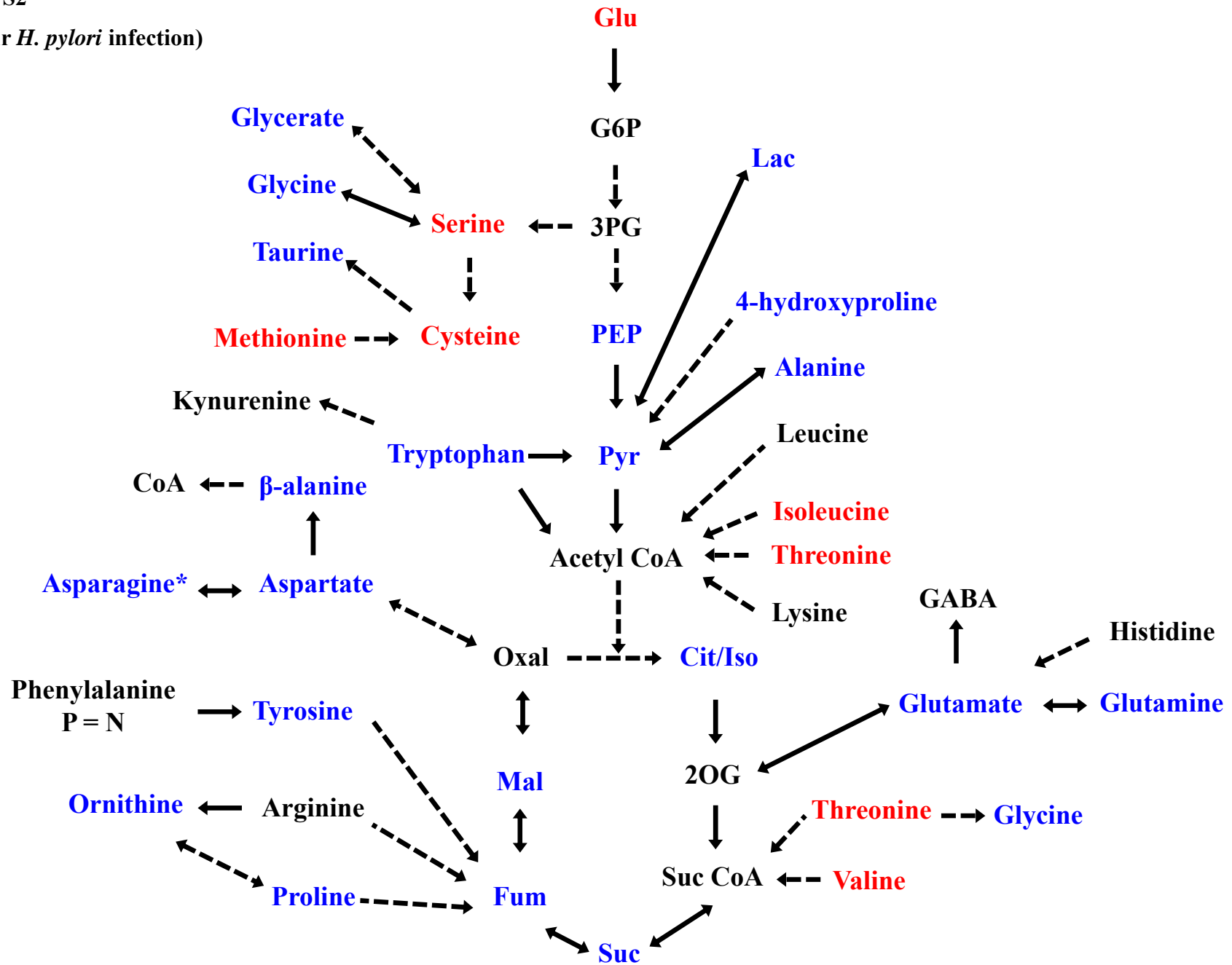


Figure S2

(6-hour *H. pylori* infection)

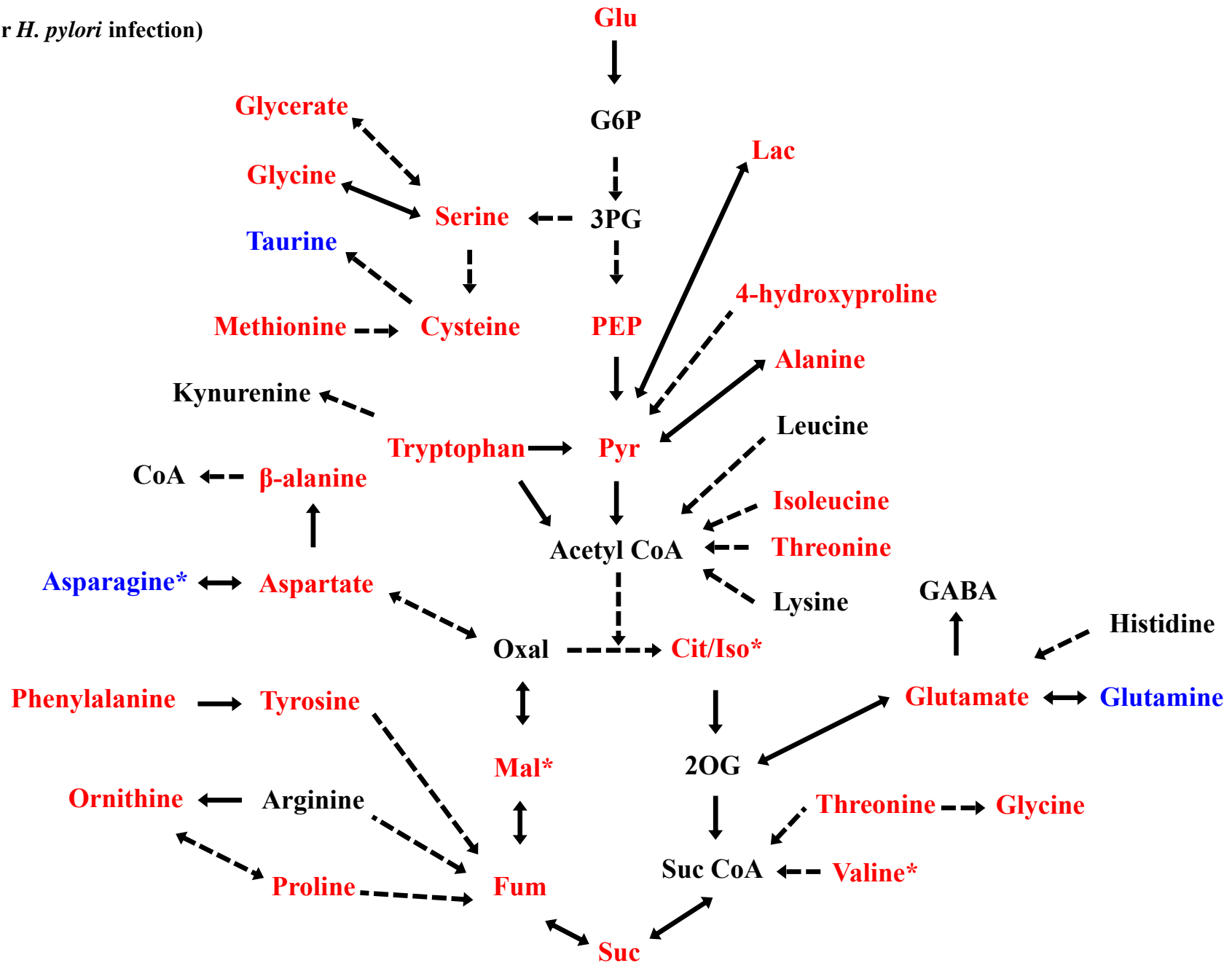


Figure S2

(12-hour *H. pylori* infection)

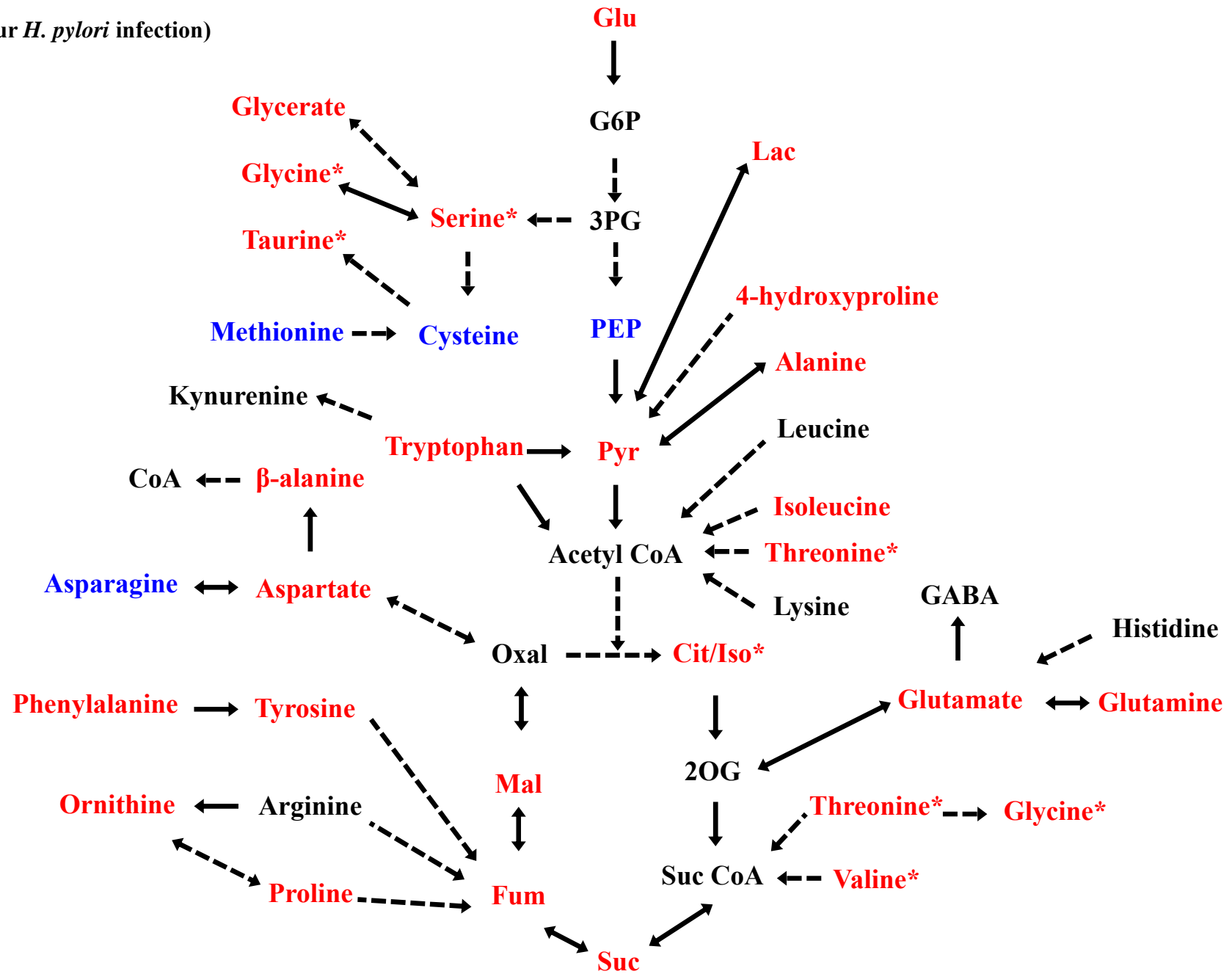
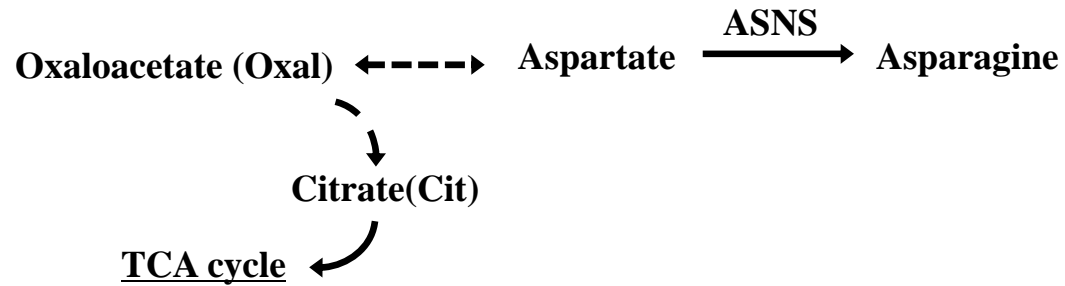


Figure S2. Alterations in the metabolic pathways of *H. pylori*-infected AGS cells seen at 2, 6, and 12 hour post-infection

AGS cells were infected with *H. pylori* (ATCC43504) for 2, 6, or 12 hours and then were subjected to evaluations of their metabolite levels based on the TCA cycle, amino acid metabolism, and the associated pathways. Asterisks indicate significant differences ($P < 0.05$) between the *H. pylori*-infected AGS cells and uninfected controls. The Student's t-test was used for comparisons between the two groups. The metabolites with black text could not be detected in our GC/MS-based metabolomic analysis. Red and blue text indicate that the level of the metabolite was higher and lower, respectively, in the *H. pylori*-infected AGS cells than in the uninfected controls.

ASNS-related metabolic pathways



IDH-related metabolic pathways

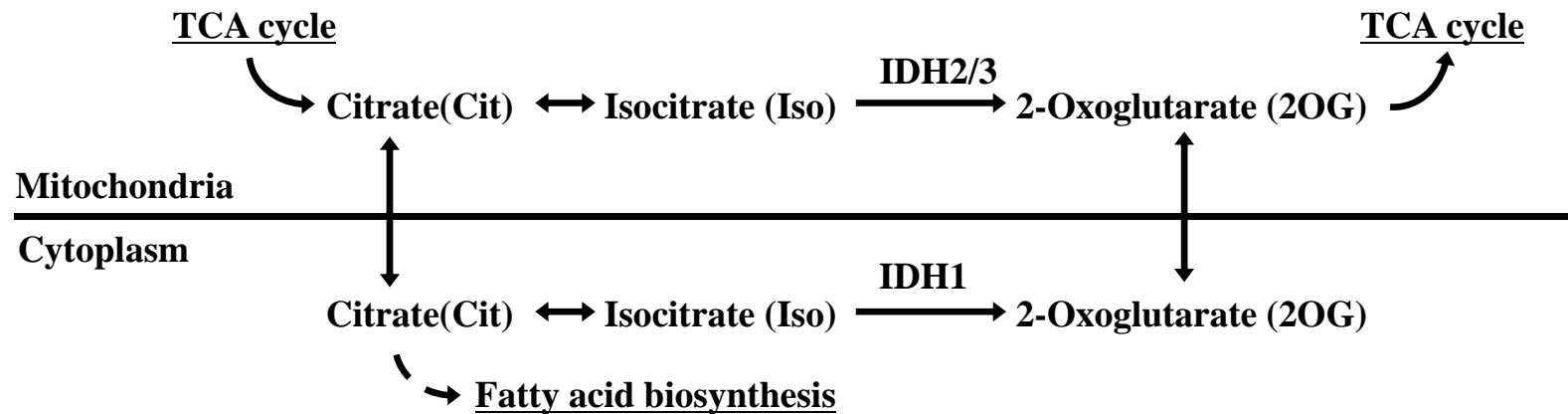


Figure S3. ASNS and IDH-related metabolic pathways